International Journal of Biological Macromolecules 79 (2015) 95–102

Contents lists available at ScienceDirect

International Journal of Biological Macromolecules

journal homepage: www.elsevier.com/locate/ijbiomac

Hollow chitosan/alginate nanocapsules for bioactive compound delivery

Melissa C. Rivera, Ana C. Pinheiro, Ana I. Bourbon, Miguel A. Cerqueira, António A. Vicente*

Centre of Biological Engineering, University of Minho, Campus de Gualtar, 4710-057 Braga, Portugal

ARTICLE INFO

Article history:
Received 20 October 2014
Received in revised form 19 February 2015
Accepted 3 March 2015
Available online 20 April 2015

Keywords:
Biodegradable polysaccharides
Multilayer
Chitosan
Alginate
Functional compounds

ABSTRACT

This work aimed at the development of biodegradable nanocapsules as carriers of two bioactive compounds, 5-aminosalycilic acid and glycomacropeptide. Nanocapsules were produced through layer-by-layer (LbL) deposition of chitosan (CH) and alginate (ALG) layers on polystyrene nanoparticles. The bioactive compounds were incorporated on the third layer of the nanocapsules being its encapsulation efficiency and release behaviour evaluated.

The LbL deposition process, stability, morphology and size of the multilayer nanocapsules were monitored by means of zeta potential and transmission electron microscopy (TEM). The bioactive compounds release from the CH/ALG nanocapsules was successfully described by a mathematical model (linear superimposition model – LSM), which allowed concluding that bioactive compounds release is due to both Brownian motion and the polymer relaxation of the CH/ALG layers.

Final results demonstrated that the synthesized LbL hollow nanocapsules presented spherical morphology and a good capacity to encapsulate different bioactive compounds, being the best results obtained for the system containing 5-aminosalycilic acid (with an encapsulation efficiency of approximately 70%).

CH/ALG multilayer nanocapsules could be a promising carrier of bioactive compounds for applications in food and pharmaceutical industries.

1. Introduction

Over the last decade, the potential use of nanotechnology has been growing in industries such as food [1] and pharmaceutical [2]. The design of micro-/nanostructures has been receiving much attention, being these structures widely applied as carrier/delivery systems of bioactive compounds (BCs) [3], where the BC benefits from an encapsulation procedure that slows down or/and prevents degradation processes until the product is delivered at the desired target (e.g. colon, stomach and small intestine) [4], thus enhancing their therapeutic effect.

Layer-by-layer (LbL) technique turned into a widely used method for the preparation of different multilayer nanostructured systems [5]. This technique consists of the alternated deposition of oppositely charged polyelectrolytes around a charged template. Multilayer nanocapsules can be obtained using a colloidal template, such as polystyrene nanoparticles, melamine formaldehyde and gold nanoparticles [6,7]. Then, at the end of the LbL deposition process, the templates is removed to obtain hollow capsules [3], which can be applied in various fields [8]. One example is their use to carry, protect and deliver bioactive compounds (BCs) or functional ingredients (e.g. drugs, antimicrobials, antioxidants and flavourings) to a specific site of action [9]. Also, this technique is an inexpensive, highly adaptable and easy solution-based assembly method, thus allowing materials to be designed and assembled with tailored properties and nanoscale precision [10].

Different strategies have been envisaged for bioactive compounds loading into LbL multilayer nanocapsules: (i) preloading the BC either in or onto the template, (ii) incorporating the BC with the layers during multilayer assembly, or (iii) post-loading the cargo into preformed capsules [10]. Glycomacropeptide (GMP) is a C-terminus portion (f 106–169) of kappa-casein (milk protein) released in whey during cheese making by the action of chymosin [11]. This peptide is known for its several beneficial biological properties, such as prevention of dental caries, zinc absorption and bacterial inhibition [12]. 5-Aminosalicylic acid (5-ASA) is an anti-inflammatory drug that has been employed for several years in the treatment and remission of inflammatory bowel disease (IBD),

* Corresponding author.
E-mail address: avicente@deb.uminho.pt (A.A. Vicente).

http://dx.doi.org/10.1016/j.ijbiomac.2015.03.003
0141-8130/

among which ulcerative colitis and Crohn's disease are the most diffuse and important [13].

In this study, GMP and 5-ASA, were used as bioactive compound models and incorporated in nanocapsules during multilayer assembly. Moreover oppositely charged biopolymers such as chitosan (CH) and alginate (ALG) have been used in the formation of hollow nanocapsules. Chitosan is a linear cationic polysaccharide composed of randomly distributed β-(1-4)-linked D-glucosamine (deacetylated unit) and *N*-acetyl-D-glucosamine (acetylated unit) and it is obtained via alkaline deacetylation of chitin [14]. Alginate is a natural anionic polysaccharide, soluble in water and extracted from marine brown algae (Phaeophyta) by treatment with aqueous alkali solutions [15]. This polysaccharide is now known for being a whole family of linear copolymers containing blocks of uronic acids, L-guluronic acid (G) and D-mannuronic acid (M), where the relative amount of the uronic acid monomers as well as their sequential arrangement along the polymer chain differs widely, depending on the origin of the alginate [16].

There has been a great interest in the study of the behaviour of LbL nanocapsules as drug delivery systems in different areas [17]. Therefore, it is of significant importance to develop nanocapsules capable of encapsulating different BCs and evaluate their behaviour during BC release.

In order to achieve this goal, the main objectives of this work were the development and characterization of CH/ALG multilayer hollow nanocapsules trough LbL deposition and evaluated their potential use as carrier of different BCs. GMP and 5-ASA (used BCs) were incorporated into the nanocapsules and their encapsulation efficiency and release behaviour was assessed.

2. Materials and methods

2.1. Materials

Chitosan (deacetylation degree ≥95%) was purchased from Golden-Shell Biochemical Co., Ltd. (Zhejiang, China) and sodium alginate from Manutex RSX, Kelco International, Ltd. (Portugal). 5-Aminosalicylic acid with a mass fraction purity of 99% was purchased from Sigma–Aldrich (St. Louis, USA). Commercial glycomacropeptide (GMP) was obtained from Davisco Food International, Inc. (Le Sueur, MN, USA). Sodium hydroxide and hydrochloric acid at 37% were obtained from Riedel-de Haen (Germany). Lactic acid (90%) was purchased from Merck (Germany). Hanks balanced salt solution (HBSS) was obtained from Invitrogen (Gibco, Invitrogen Corporation, Paisley, UK). Polystyrene nanoparticles were purchased from Polysciences, Inc. (Warrington, PA, USA). All samples were prepared with distilled water purified to a resistance of 15 MΩ cm.

2.2. Layer-by-Layer assembly

2.2.1. Preparation of polyelectrolyte solutions

Polyelectrolyte solutions were prepared dissolving sodium alginate (ALG) in distilled water with agitation using a magnetic stirrer (at 200 rpm) during 2 h at room temperature (20 °C). Chitosan (CH) solution (1 mg/mL) was prepared in 1% of lactic acid, through the same methodology used for the ALG solution (1 mg/mL). The pH of polyelectrolyte solutions was adjusted with 0.1 mol/L sodium hydroxide (NaOH) or with 0.1 mol/L lactic acid solutions.

2.2.2. Assessment of solutions charge

In LbL deposition the pH of solutions (CH, ALG, 5-ASA and GMP) must be adjusted in order to guarantee a correct electrostatic interaction between the layers and/or components of the capsule, i.e. between PS nanoparticles, 5-ASA, GMP, ALG and CH layers. Likewise, in order to achieve the aforementioned conditions, it is crucial to choose the adequate pH for each solution (e.g. below or above the pK_a and/or p*I*), where the solutions should exhibit opposite surface charges (positive or negative).

2.2.2.1. Chitosan and alginate. Chitosan (CH) and alginate (ALG) are weak polyelectrolytes, meaning that their dissociation degree depends strongly on the solution pH (below or above the pK_a). It was previously reported that when the pH of ALG solution is below or close to the pK_a value (~3.4–4.4), a drastic decrease in the ionization degree of ALG macromolecules is observed leading to a lack of sufficient charge, which would difficult its self-assembly deposition [6]. In the case of CH, it is only soluble in acidic solutions, where the pH value is already distant from its pK_a (6.2–7.0) [2]. Based on this information, the pH values for ALG and CH deposition were fixed at 6.0 and 3.0, respectively. The behaviour of CH and ALG was therefore assessed using these pH values in order to ensure their polycation and polyanion behaviour, respectively.

2.2.2.2. Model bioactive compounds. Glycomacropeptide (GMP) and 5-aminosalycic acid (5-ASA) were chosen as bioactive compound models. GMP solution (1 mg/mL) was prepared dissolving GMP in distilled water with agitation using a magnetic stirrer (at 200 rpm) during 2 h at room temperature (20 °C). 5-ASA solution (1 mg/mL) was prepared in 2% of lactic acid, through the same methodology used for the GMP solution.

Being assembled onto a negative charged polyelectrolyte (ALG), BCs must present a positive surface charge in order to allow electrostatic interactions between layers. This is achieved by choosing the pH value for GMP and 5-ASA solutions, which corresponds to the highest positive zeta potential value. Regarding GMP, it was previously reported [18] that the solution exhibits a positive and maximum zeta potential value at pH = 2, while for 5-ASA, preliminary experiments showed that pH = 2.3 is the most adequate value to obtain those conditions (results not shown). The pH of bioactive compound solutions was adjusted with 0.1 mol/L sodium hydroxide (NaOH) or with 0.1 mol/L lactic acid solutions.

2.2.3. Preparation of chitosan/alginate multilayer nanocapsules

Multilayer nanocapsules have been prepared in aqueous media by LbL deposition of CH and ALG onto PS nanoparticles according to Ye et al. [6], with some modifications:

(1) PS nanoparticles aqueous dispersion (0.5 mg/mL) was used as the template.
(2) First layer was deposited with the addition of 1 mL of CH solution into 0.5 mL of PS nanoparticles solution. The mixture was incubated at room temperature, for 10 min under gentle agitation.
(3) The excess of polyelectrolyte was removed by two repeated cycles of centrifugation (18,625 × *g* for 20 min, MIKRO 120, Hettich, Germany) with consequent removal of supernatant and redispersion in water (pH 7), discarding the unadsorbed CH in the suspension. In addition, sonication was used to improve the dispersion of the capsules in the solution by preventing their fast agglomeration [19,20]. Moreover, sonication also allows exploiting maximum surface area for subsequent polyelectrolyte deposition [21]. For this purpose, sonication (40 kHz, 30 min) was used after the cycles of centrifugation.
(4) The following ALG layer was deposited with 1 mL ALG solution (1 mg/mL) using the same procedure described in steps 2 and 3.

This procedure was repeated until three CH/ALG layers were assembled onto PS nanoparticles (Fig. 1), resulting in PS-$(CH\text{-}ALG)_3$ nanocapsules. All sets of experiments were made at least in duplicate.

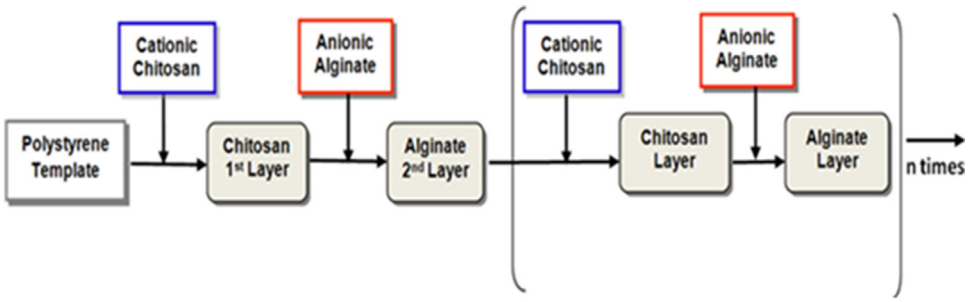

Fig. 1. Preparation of CH/ALG multilayer nanocapsules (without the bioactive compound), $n = 2$.

2.2.4. Incorporation of model bioactive compound

Model bioactive compounds, 5-aminosalicylic acid (5-ASA) and glycomacropeptide (GMP), were incorporated into the multilayered CH/ALG nanocapsules during LbL assembly procedure. As deposition on the 1st layer (PS-BC-CH-ALG-CH-ALG-CH) did not show reproducibility in terms of deposition (assessed through zeta potential measurements, data not shown), both BCs were deposited in the third layer, forming PS-CH-ALG-BC-CH-ALG (Fig. 2).

Briefly, 1 mL aqueous BC solution (1 mg/mL) was added to 1 mL of pre-formed PS-(CH-ALG) nanocapsule solution. Then additional CH/ALG layer was deposited, using the same concentrations and procedure described in Section 2.2.3.

2.2.5. Core removal

For core removal, the multilayer nanocapsules were dipped in tetrahydrofuran (THF) for 12 h, and then the suspension was centrifuged at 18,625 × *g* for 20 min (MIKRO 120, Hettich, Germany). This dissolution process was repeated twice to ensure complete removal of the PS core. Then the resulting capsules were washed three times with distilled water and centrifuged to remove the residual THF, and finally redispersed in distilled water. As final step, the hollow capsules were sonicated for 30 min. Hollow nanocapsules samples were kept at 4 °C before characterization.

2.3. Nanocapsules characterization

2.3.1. Zeta potential measurements

The electrophoretic mobility was determined by dynamic light scattering (DLS) with a Malvern Zetasizer, Nano ZS particle characterization system (Malvern Instruments Limited, UK), using a He–Ne laser (wavelength of 633 nm) at an angle of 17° which is combined with the reference beam to analyze the samples. Zeta potential values were calculated by the Smoluchowski's relation/approximation, converting electrophoretic mobility to zeta potential values. The measurements (three readings for each assay) were performed in a folded capillary cell. The assays were performed in triplicate, so the results are given as the average ± standard deviation of the nine values obtained.

2.3.2. Size evaluation

The average particle size and morphology of capsules were examined using a Zeiss 902 transmission electron microscope (TEM) operating at a voltage of 80 kV. The aqueous dispersion of the capsules was drop-cast onto a carbon coated copper grid and grid was air dried at room temperature (20 °C) before loading into the microscope (direct deposition).

2.3.3. Determination of encapsulation efficiency

Encapsulation efficiency (*EE*%) was determined by measuring the amount of BC which was not encapsulated. Briefly, after the deposition of the BC, 0.5 mL of nanocapsules solution was placed in the Eppendorf Amicon® Ultra 0.5 centrifugal filters with 10 kDa cut-off and centrifuged at 18,625 × *g* for 10 min. This allowed separating the BC encapsulated in nanocapsules, being the unabsorbed BC (free BC) in the supernatant/filtrated solution estimated by UV/vis absorbance at 300 nm [22] and at 230 nm [23] for 5-ASA and GMP, respectively. The previous procedure was performed twice since the unabsorbed BC was removed by two repeated cycles of centrifugation. The BC encapsulation efficiency (*EE*%) was calculated from the following equation (1) [24]:

$$EE\% = \frac{\text{Total BC} - \text{Free BC}}{\text{Total BC}} \times 100 \quad (1)$$

All measurements were performed in triplicate. Additionally the concentration values of BC (mg/mL) were determined using a standard calibration equation.

2.3.4. Determination of BC release profile

Release profiles of BC were determined using the dialysis method. About 2 mL of nanocapsules aqueous suspension were added into a sealed dialysis bag with a molecular weight cut-off (MWCO) of 3500 Da for 5-ASA and 25,000 Da for GMP (Cellu-Sep H1, Membrane filtration products, USA); the sealed bag was immersed into 40 mL of Hanks Balanced Salt Solution (HBSS – pH 7.0) at 37 °C. The release medium was continuously stirred at 60 rpm. At regular time intervals, 1 mL of released medium was taken, and to maintain the original volume, 1 mL of fresh HBSS was added into the medium after each sampling. BC concentration was followed through time by measuring the absorbance (Elisa Biotech Synergy HT) at

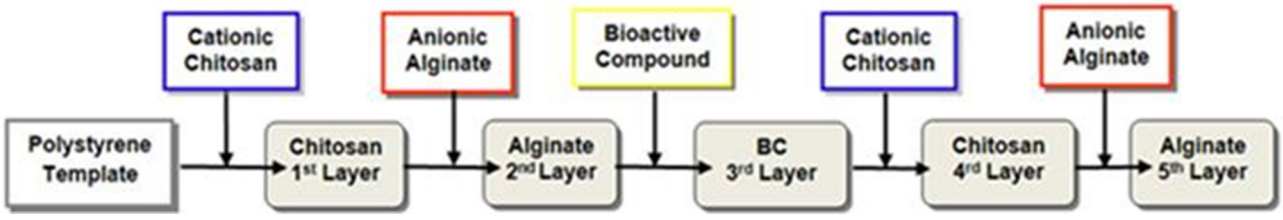

Fig. 2. Pre-loading of the bioactive compound (BC) in third layer of the CH/ALG multilayer nanocapsule.

appropriated wavelengths: 300 nm and 230 nm, which correspond to the maximum absorbance peak of 5-ASA and GMP, respectively. All the experiments were performed in triplicate, and the average values were taken.

2.3.4.1. Mathematical modelling. When immersed in liquid media, there are different mechanisms that govern compounds release from bio-polymeric systems [25]. These mechanisms associated with compounds release can be generally classified in different types: (i) Fickian diffusion, described as a substantially stochastic phenomenon (related to Brownian motion), where the governing factor for transport mechanism is exclusively a concentration gradient; (ii) Case II transport (polymeric relaxation), where the dominant mechanism for transport is polymer relaxation driven by the distance of the local system from the equilibrium; and (iii) anomalous transport, a coupling of diffusion and polymeric relaxation.

In order to describe the transport properties of BC inside a polymeric matrix, several mathematical approaches have been proposed [26]. The Linear Superimposition Model (LSM) is one of the ways to quantitatively describe the Fickian diffusion and Case II transport [27]. LSM approach was reported in some transport studies of bio-polymeric systems [23], including at the nanoscale level [28].

This approach assumes that the mass transport within the polymeric system can be described by the sum of the molecules transported due to Brownian motion with the molecules transported due to polymeric relaxation [27]. Fickian contribution ($M_{t,F}$) can be described by the solution of Fick's second law for a "uniform sphere model" with constant boundary conditions (Eq. (2)):

$$M_{t,F} = M_{\infty,F}\left[1 - \frac{6}{\pi^2}\sum_{n=1}^{\infty}\frac{1}{n^2}\exp\left(-n^2\cdot\frac{4\pi^2 D}{d^2}\cdot t\right)\right] \quad (2)$$

where $M_{\infty,F}$ is the amount of compound released at equilibrium in the unrelaxed polymer, D is the diffusion coefficient, and d is the particle diameter.

As for relaxation process contribution ($M_{t,R}$), it is driven by the swelling ability of the polymer and is then related to the dissipation of stress induced by the entry of the penetrant and can be described as a distribution of relaxation times (i), each following a first order-type kinetic equation:

$$M_{t,R} = \sum_i M_{\infty,i}\left\lfloor 1 - \exp(k_{R_i}t)\right\rfloor \quad (3)$$

where $M_{\infty,i}$ is the equilibrium sorption of the i relaxation process, and i is respective relaxation rate constant. The above equation can be simplified, because in most of the cases, only one polymer relaxation ($i = 1$) influences transport [25]. Taking the above conditions into account, LSM approach for compound release can be described/expressed as follows:

$$M_t = M_{\infty,F}\left[1 - \frac{6}{\pi^2}\cdot\exp\left(-\frac{4\pi^2 Dt}{d^2}\right)\right] + M_{\infty,R}\left\lfloor 1 - \exp(k_R t)\right\rfloor \quad (4)$$

This "general" model can then be used to describe pure Fickian ($M_{\infty,F} \neq 0$ and $i = 0$); anomalous ($M_{\infty,F}$ and $i \neq 0$) or Case II ($M_{\infty,F} = 0$ and $i \neq 0$) transport.

2.4. Statistical analyses/procedures

All data were expressed as mean ± standard deviation (SD) from at least three values. One-way analysis of variance (ANOVA) was employed to assess the statistical significance of results between groups. Experimental results were considered statistically significant at 95% confidence level ($p < 0.05$). All analyses performed using SigmaStat® 3.5 software (trial version).

2.4.1. Non-linear regression analysis

The equations mentioned along the text were fitted to data by non-linear regression analysis, using a package of STATISTICA™7.0 (Statsoft. Inc., USA). The Levenberg–Marquadt algorithm for the least squares function minimization was used. The quality of the regressions was evaluated on the basis of the determination coefficient, R^2, the squared root mean square error, RMSE (i.e., the square root of the sum of the squared residues (SSE) divided by the regression degrees of freedom) and residuals visual inspection for randomness and normality. R^2 and SSE were obtained directly from the software. The precision of the estimated parameters was evaluated by the Standardized Halved Width (SHW %), which was defined as the ratio between the 95% standard error (obtained from the software) and the value of the estimate.

3. Results and discussion

3.1. Development of chitosan/alginate hollow nanocapsules

3.1.1. Evaluation of chitosan and alginate deposition

LbL deposition is a technique mainly governed by electrostatic interactions, so it is important to assess the charge density of CH and ALG polyelectrolytes in order to guarantee a successful interaction between the surface of PS nanoparticles (with a known negative charge density) and CH layer and between the subsequent CH/ALG layers. Therefore to confirm the opposite charges of CH and ALG solutions, their zeta potential values were determined. It was observed that CH (pH = 3) and ALG (pH = 6) solutions present superficial charges of +48.20 ± 7.00 and −58.28 ± 4.48, respectively, which means that they can interact by electrostatic forces. Obtained values are in agreement with the ones obtained elsewhere [25,29].

Fig. 3 shows the zeta potential values during the CH/ALG deposition process. Zeta potential alternates according to the last adsorbed outer layer (n) on PS nanoparticles, starting from a negative zeta potential of the PS nanoparticles (−38.47 ± 8.08 mV), the surface of which turns to a positive value (+67.6 mV) after the deposition of the 1st layer (CH). Subsequently, when the anionic polyelectrolyte (ALG) was added to the solution the zeta potential value becomes negative again (−49.3 mV) (Fig. 3). During the overall process, zeta potential values oscillate between +60 and +70 mV after polycation adsorption, and around −40 to −50 mV

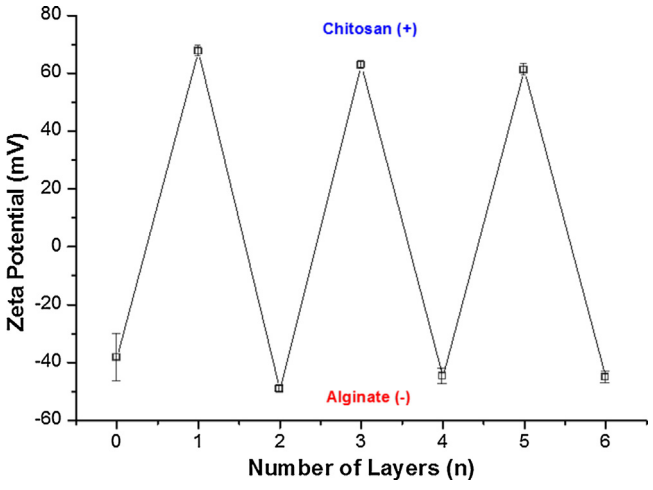

Fig. 3. Zeta potential values as function of the number of deposited layers (n).

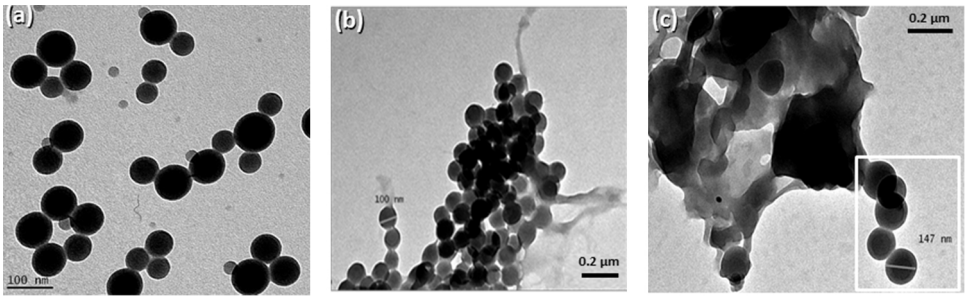

Fig. 4. TEM images of (a) PS nanoparticles, (b) chitosan/alginate multilayer nanocapsules and (c) respective hollow nanocapsules.

after polyanion adsorption. This constant alternated switching (Fig. 3) is an indicative of the successful self-assembly of the polyelectrolytes CH and ALG onto PS nanoparticles [30].

Moreover, zeta potential constant values show that no aggregation and precipitation occurs during the deposition process, otherwise the mobility of the colloid particle should be decreased, resulting in a decrease of zeta potential values [6]. In addition, detailed evaluation of the morphology and size distribution of PS nanoparticles and PS-$(CH\text{-}ALG)_3$ nanocapsules were performed by TEM (Fig. 4). Fig. 4a shows that PS nanoparticles are spherical and smooth, and present an average diameter of 90 nm. After CH/ALG assembly, the produced nanocapsules (PS-$(CH\text{-}ALG)_3$) maintained a spherical shape and have a diameter of approximately 100 nm (Fig. 4b), which is larger than that of the PS nanoparticles, 90 nm (obtained by TEM), thus indicating that the average thickness of the deposited layers is of ca. 5 nm. The increase of the nanocapsules diameter is ascribed to the deposition of three CH/ALG bilayers on the surface of PS nanoparticles [31]. Ye et al. [6] reported a similar behaviour, where the deposition of five bilayers of CH/ALG resulted in an average thickness of 13 nm.

TEM analysis after core removal revealed a visible aggregation of the nanocapsules (Fig. 4c). One possible explanation can be based on the effect of THF during core removal, damaging some of the nanocapsules. Nevertheless a minority maintained the spherical geometry, as can be seen in Fig. 4c (inset), demonstrating the formation of intact hollow nanocapsules with a diameter of approximately 147 nm, larger than the corresponding nanocapsules before core removal (Fig. 4b). This increase in the diameter suggests the swelling of the nanocapsules during PS core removal and rinse of THF with pure water [6]. The surface charge of hollow nanocapsules was measured and the results showed that nanocapsules maintained their negative surface charge (-37.5 ± 5.9 mV), indicating that the last ALG layer has been preserved during the core removal process. Additionally, since all the zeta potential values measured exhibit absolute values higher than 30 mV, it can be said that the $(CH/ALG)_3$ nanocapsules formed are very stable [32].

3.1.2. Incorporation of bioactive compounds (BCs)

The incorporation of BC in CH/ALG multilayer nanocapsules was performed for further evaluation of efficiency and release behaviour of BC from CH/ALG multilayer nanocapsules. The pH value of both 5-ASA (pH = 2.3) and GMP (pH = 2) solutions was chosen based on the electrostatic values that lead to a high interaction between BC and ALG layer, in order to achieve a high deposition of BC on the CH/ALG nanocapsules. Thus these conditions lead to positive zeta potential values of 22.54 ± 4.80 and 11.75 ± 2.98, respectively in 5-ASA and GMP solutions. Therefore, both BC meet the required conditions for being incorporated in the 3rd layer of multilayer nanocapsules, leading to the formation of PS-CH-ALG-BC-CH-ALG nanocapsules.

3.1.2.1. Glycomacropeptide and 5-aminosalicylic acid. The stepwise growth of multilayers onto PS nanoparticles was monitored by measuring the zeta potential of the nanoparticles after each deposition step (Fig. 5). When BC was added on the 2nd layer (ALG layer) it resulted in a negative value of zeta potential, for both GMP (Fig. 5a) and 5-ASA (Fig. 5b).

Despite the lack of reversal in zeta potential signal, the value obtained after BC addition was less negative when compared to the previous value of the capsule solution (−62 mV). Typically, this fact indicates that an electrostatic complex had been formed [33], although with incomplete coverage of the nanoparticle surface. Presumably the BCs (GMP and 5-ASA) were "partially" adsorbed, however they were not capable of forming a layer dense enough to completely cover the charges from the preceding ALG layer. This behaviour has been previously observed by other authors [34] for CH/ALG multilayered nanostructures assembled by LbL technique. Corredig et al. [35] reported that most of the complexes between caseins (GMP) and polyelectrolytes (such as CH) are formed close to or below the p*I* of the proteins. This is the case of GMP solution used that presents a pH value of 2 (pH value below its p*I*), which means that in this conditions GMP will be more prone to electrostatic interact with ALG layer.

Following the addition of BC, a CH layer was added. CH was chosen to coat the BC due to its high positive charge in contrast to the negative surface charge of the BC layer. The adsorption of CH layer was confirmed by the increase of the zeta potential values on the capsule surface, i.e. the BC coated with CH exhibited positive zeta potential values of 56.63 ± 4.48 and 51.48 ± 6.09 mV, for 5-ASA and GMP, respectively. After the last assembled layer (ALG) the zeta potential values turned negative again (Fig. 5), indicating the successful deposition of the 5th layer onto the nanocapsules.

Overall, these results (Fig. 5) showed that after each adsorption of polyelectrolyte, the oppositely charged surface is not just compensated, but strongly over-compensated. The phenomenon of over-compensation plays a crucial role in LbL assembly and is considered as the indicative of progression during the multilayer formation [36]. Moreover, considering the absolute value, the majority of the zeta potential values observed are particularly high (>30 mV), being an indicative of high stability of the nanocapsules produced [37]. This behaviour was observed when both BC models were incorporated on the nanocapsules, suggesting that the configuration adopted PS-CH-ALG-BC-CH-ALG is suitable for encapsulating different bioactive compounds.

To provide direct evidence of the LbL deposition and size, the resulting nanocapsules loaded with GMP and 5-ASA were observed by TEM (Fig. 6a and b). The obtained nanocapsules maintained the spherical shape and no rupture of the nanocapsule wall was observed. In addition, the nanocapsule diameter increased up to 110 nm after the deposition process, which may be ascribed to the adsorption of the polyelectrolytes around the PS nanoparticles. Together, the aforementioned results indicate that there was a

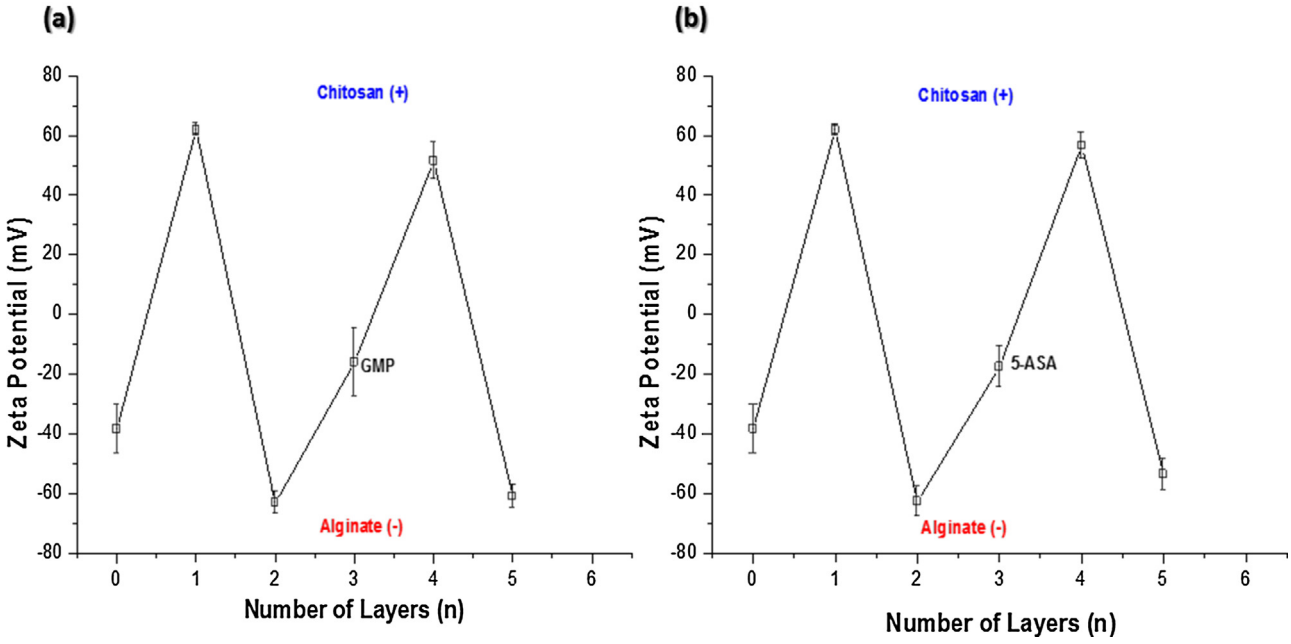

Fig. 5. Zeta potential values as function of the number of deposited layer (*n*). (a) GMP and (b) 5-ASA deposition.

stepwise growth of CH/ALG multilayer around the BC, pointing out to the formation of multilayer nanocapsules (PS-CH-ALG-BC-CH-ALG) with a regular, spherical shape and a solid dense structure (Fig. 6a and b).

3.1.3. Hollow nanocapsules

Hollow nanocapsules can be obtained by dissolving the core (PS nanoparticles) after the LbL deposition procedure, as previous reported in other CH/ALG multilayer structures [38,39]. Before core removal the measured zeta potential values were -61.03 ± 3.85 and -53.7 ± 5.16 mV for nanocapsules loaded with GMP and 5-ASA, respectively (Fig. 5). The negative charge was attributed to the carboxyl groups of ALG, the outermost surface layer of the nanocapsules [40]. Then, after core removal, a decrease in the absolute value of zeta potential was observed, for both GMP (−42 mV) and 5-ASA (−51 mV) nanocapsules. These changes in zeta potential after removal of PS by THF incubation are consistent with the literature [41]. The exact reason that explains this decrease of zeta potential remains speculative. However, it can be explained by the THF effect in the core removal that could have damaged some of the nanocapsules, causing a decrease on their surface charge. It is worth to mention that despite the decrease in zeta potential values, the nanocapsules surface maintained a negative value.

As for TEM analysis, it showed that the hollow nanocapsules (CH-ALG-BC-CH-ALG) obtained after core removal did not show a regular size distribution but a variety of sizes (Fig. 6c and d). Despite this variety of size, the hollow nanocapsules exhibit a high surface charge (i.e. higher than −30 mV) that confirms their stability, as indicated in previous studies [37].

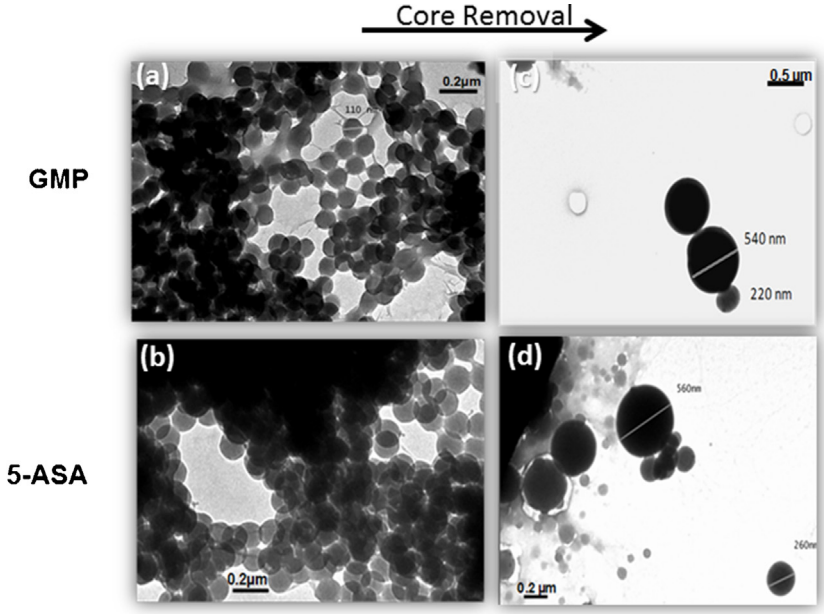

Fig. 6. TEM images of chitosan/alginate multilayer nanocapsules loaded with (a) GMP, (b) 5-ASA and respective hollow nanocapsules (c and d).

3.1.4. Encapsulation efficiency of the bioactive compounds

Encapsulation efficiency (*EE*%) is an important parameter for assessing the capacity of the capsule to retain the BC, and in order to evaluate the release of BC from nanocapsules. Moreover, it is known that the number of deposited layers and the encapsulated BC have influence on *EE*% multilayer microcapsules [30].

The *EE*% for GMP and 5-ASA deposition on 3rd layer of the CH/ALG multilayer nanocapsules was determined. The *EE*% of 5-ASA and GMP was 70.91 ± 0.14 and 49.45 ± 9.22%, respectively.

The higher *EE*% of 5-ASA (when compared to GMP), can be explained by its surface charge (22.54 ± 4.80); in this case the electrostatic interaction between BC and ALG layer hampered the 5-ASA loss during the deposition, rinse and centrifugation processes when incorporating the subsequent polyelectrolyte layers of CH and ALG. As for GMP, that exhibits a lower surface charge (11.75 ± 2.98), its diffusion into solution during polyelectrolyte deposition processes is somewhat facilitated [40], thus resulting in a loss of peptide and a lower amount of it encapsulated inside CH/ALG nanocapsules.

Moreover, the obtained value of *EE*% is higher when compared with other studies that encapsulate 5-ASA [42]. Loaded 5-ASA into Eudragit S100 (EU S100) nanoparticles achieved an encapsulation efficiency of 60.51% [43]. Nanoparticles of poly (D,L-lactic-co-glycolic acid) containing 5-ASA presented an encapsulation efficiency of 44.7%, while Karewicz et al. [44] encapsulated 5-ASA in CH–κ-carrageenan coated ALG microbeads with an encapsulation efficiency of 20%. However, other studies also reported higher values of encapsulation efficiency, in particular Aguzzi et al. [45] prepared microspheres that also rely on the interaction between 5-ASA and CH, obtaining this way *EE*% values higher than 90%.

3.1.5. Bioactive compounds release of chitosan/alginate nanocapsules

The release properties of the BC models (GMP and 5-ASA) from the hollow CH/ALG multilayer nanocapsules (CH-ALG-BC-CH-ALG) were determined by measuring the concentration of the GMP/5-ASA compound in the release media as a function of time.

In order to evaluate the transport mechanisms involved in the BC release from CH/ALG nanocapsules to the liquid medium (HBSS), the LSM model (Eq. (4)) was fitted to the experimental data (Figs. 7 and 8).

Experimentally, GMP and 5-ASA release followed a similar profile: an initial burst, followed by a decrease in the release rate, and at the end a stagnant release phase (Figs. 7 and 8).

From the regression analysis results (Table 1), it can be observed that this model presents a good regression quality (adjusted $R^2 > 0.96$), for both GMP and 5-ASA experimental release data. Therefore, it demonstrates that LSM model is an appropriated mathematical model to represent the transport mechanism involved in BC release from the hollow CH/ALG multilayer nanocapsules. Although RMSE is lower and the quality of estimated parameters (based on SHW (%)) is better when the fitting is made to experimental data of GMP, indicating that LSM model is more accurate in representing GMP release.

Moreover, the results presented in Table 1, allowed concluding that GMP and 5-ASA release from CH/ALG nanocapsules was due to both Fick's diffusion and relaxation phenomena (anomalous transport, anomalous transport, and $i \neq 0$), where one main relaxation seems to be enough to describe the release profile of both BCs. The results are in agreement with the hydrophilic nature of CH and ALG polymers/layers; once when immersed in liquid media (HBSS), these polymers gradually start to hydrate, causing relaxation of the polymers chain [46]. The effects of the environmental conditions (i.e. temperature and pH) on the quantity (mass) of 5-ASA and GMP released and on the release rate can be extremely relevant for these systems' application. In this context, the release profile/behaviour and estimated parameters (Table 1) at 37 °C and pH = 7.0 (HBSS), could provide a good insight on the behaviour of these nanocapsules within the local where BC is intended to be absorbed, the small intestine. Observing Table 1, it can be assumed that at the used temperature and pH conditions, both GMP and 5-ASA, are predominantly released due to the relaxation phenomenon ($M_{\infty,R} \gg M_{\infty,F}$).

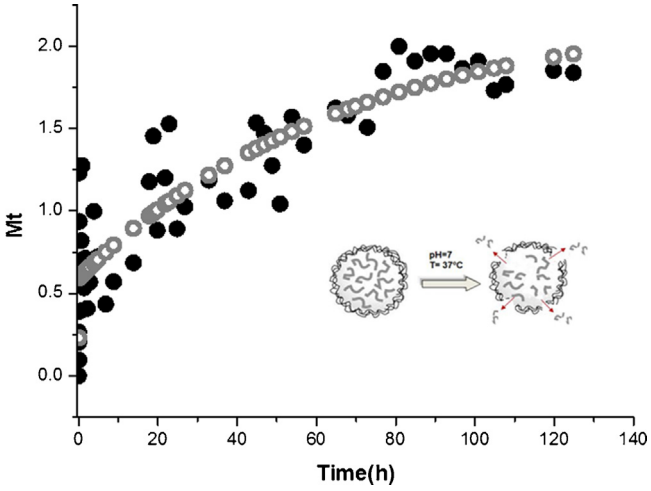

Fig. 7. Linear Superimposition Model (LSM) description of GMP release from multilayer nanocapsules (experimental results (•); model-generated values (○).

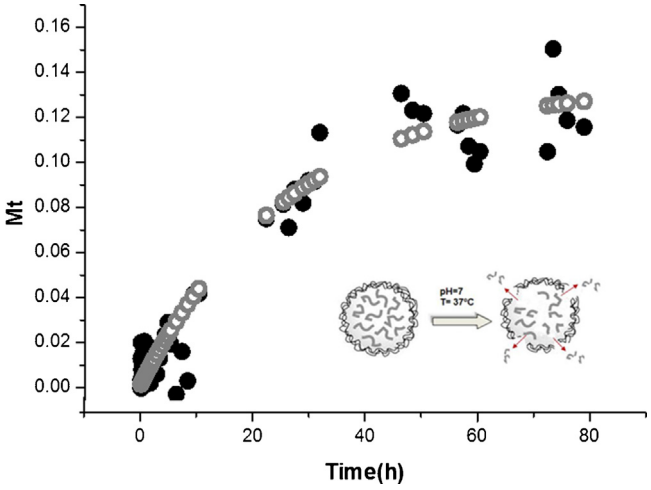

Fig. 8. Linear Superimposition Model (LSM) description of 5-ASA release from multilayer nanocapsules (experimental results (•); model-generated values (○).

Table 1
Results of fitting the Linear Superimposition Model (LSM) (modified Eq. (4)) to experimental data on BC release to liquid medium (HBSS): quality of the regression on the basis of RMSE and adjusted R^2, and estimated parameters and evaluation of estimate precision using the SHW % (in parenthesis).

	Mw[a] (kDa)	R^2	RMSE	$M_{\infty,F}$ (mg)	D (m²/s)	$M_{\infty,R}$ (mg)	K_R (s⁻¹)
GMP	20.30	0.962	6.54×10^{-2}	0.59 (17.0%)	6.38×10^{-15} (100%)	1.61 (28.2%)	1.49×10^{-2} (44.1%)
5-ASA	0.153	0.964	2.14×10^{-4}	4.43×10^{-3} (81.5%)	4.42×10^{-20} (100%)	1.30×10^{-1} (35.8%)	3.73×10^{-2} (99.9%)

[a] Molecular weight.

At pH 7, the anionic ALG in CH/ALG complex could be displaced by hydroxyl ions and CH would loose its positive charge [47]. In this context, the electrostatic interactions in the nanocapsules would be weakened, thus resulting in relaxation of the whole structure.

Also at pH 7, the behaviour of BCs can be affected; in other words, when pH is below GMP's p*I* (4–5) this molecule is positively charged [48]; as for 5-ASA, it is only positively charged for pH values ranging between 2.3 and 5. So at pH values higher than 5, such as that of the release media (HBSS, pH = 7) GMP and 5-ASA become negatively charged and the interactions between the BC and ALG layer are weaker (due to electrostatic repulsion) leading to the release of the BC. A similar behaviour was observed by Ye et al. [49] during insulin release from CH/ALG microcapsules. This decrease of electrostatic interactions (between CH, ALG and the BC) facilitates loosening of the polymer chain network and thus promotes release, again due to relaxation phenomena [25].

Moreover, observing diffusion coefficient (D) and relaxation rate (K_R) constants, it can be said that both Fick's diffusion and relaxation phenomena occur at a faster rate for GMP (Table 1). It was expected a slower rate for GMP, as it exhibits a higher molecular weight. Although the surface of GMP present a reduced positive surface charge (+11.75 mV) when compared to 5-ASA (+22.54 mV), making the interactions between GMP and ALG layer weaker (due to electrostatic repulsion). Thus, this behaviour could be ascribed to the faster release rate of diffusion and relaxation phenomena during GMP release.

The approach presented here (LSM model), which accounts for both Fickian and Case II transport effects, allows interpretation of the phenomena involved in BCs (GMP and 5-ASA) transport in the CH/ALG multilayer nanocapsules. From these results, it can be said that the transport of BC was governed by an anomalous behaviour. Similar results were found by other authors, e.g. Jager et al. [50] observed that the release mechanism behind indomethacin ethyl ester was also dominated by the anomalous transport.

4. Conclusions

One of the aims of the presented work addressed the development and characterization of CH/ALG nanocapsules, using LbL assembly technique. The first and foremost conclusion is that LbL assembly was an effective technique for the development of CH/ALG nanocapsules.

Regarding nanocapsules characterization, it was observed that they presented interesting features, namely incorporation of the BCs affected neither the integrity nor the structure of nanocapsules. Moreover the resulting nanocapsules presented a high charge on their surface (>±30 mV), which was an indicative sign of a remarkable stability. Also CH/ALG multilayer nanocapsules revealed relatively high encapsulation efficiencies, thus holding potential to be a suitable carrier for bioactive compounds encapsulated. Where encapsulation of 5-ASA (~70%) presented better results of encapsulation efficiency, when compared with encapsulation of GMP (~50%).

Based on *in vitro* BC release, the deposition of the BCs in the 3rd layer and CH/ALG complex seem to have protected both BCs, suggesting that encapsulation within the 3rd layer could hamper the immediate release of BC in biological/physiological solutions (pH = 7), such as intestinal medium. Overall, the results suggest that encapsulation of BC within the 3rd layer could be an alternative to the "traditional" loading.

As few works can be found in the release mechanisms of BC at nanoscale level, these results may contribute to an understanding of the release mechanisms in other nanosystems that present similar physical properties, suggesting that CH/ALG multilayer nanocapsule could be a promising carrier for applications in different areas, such as food and pharmaceutical industries.

Acknowledgments

The authors Ana I. Bourbon and Miguel A. Cerqueira are recipients of a fellowship (SFRH/BD/73178/2010 and SFRH/BPD/72753/2010, respectively) supported by Fundação para a Ciência e Tecnologia, POPH-QREN and FSE (Portugal). The authors thank the FCT Strategic Project PEst-OE/EQB/LA0023/2013 and the Project "BioInd – Biotechnology and Bioengineering for improved Industrial and Agro-Food processes", REF. NORTE-07-0124-FEDER-000028 Co-funded by the Programa Operacional Regional do Norte (ON.2 – O Novo Norte), QREN, FEDER. The authors also thank the COST Action FA1001.

References

[1] S. Shrivastava, D. Dash, Proc. Natl. Acad. Sci. India B: Biol. Sci. 82 (1) (2012) 29–35.
[2] T.W. Wong, U. Mandal, L.-J. Shen, Patenting Nanomedicines, Springer, Berlin/Heidelberg, 2012, pp. 345–374.
[3] M.A. Cerqueira, et al., Food Eng. Rev. 6 (1-2) (2013) 1–19.
[4] P. de Vos, et al., Int. Dairy J. 20 (4) (2010) 292–302.
[5] Y. Wang, A.S. Angelatos, F. Caruso, Chem. Mater. 20 (3) (2007) 848–858.
[6] S. Ye, et al., J. Biomater. Sci. Polym. Ed. 16 (7) (2005) 909–923.
[7] T. Pavlitschek, M. Gretz, J. Plank, J. Appl. Polym. Sci. 127 (5) (2013) 3705–3711.
[8] L. Loretta, et al., LbL Multilayer Capsules: Recent Progress and Future Outlook for Their Use in Life Sciences, Royal Society of Chemistry, 2010, pp. 458–467.
[9] K. Ariga, et al., Adv. Drug Deliv. Rev. 63 (9) (2011) 762–771.
[10] A.P.R. Johnston, et al., Multilayer Thin Films, Wiley-VCH Verlag GmbH & Co. KGaA, 2012, pp. 801–829.
[11] R. Sharma, Y.S. Rajput, B. Mann, Dairy Sci. Technol. 93 (1) (2013) 21–43.
[12] C. Thomä-Worringer, J. Sørensen, R. López-Fandiño, Int. Dairy J. 16 (11) (2006) 1324–1333.
[13] A.G. Balducci, et al., Int. J. Pharmaceut. 421 (2) (2011) 293–300.
[14] M. Rinaudo, Prog. Polym. Sci. 31 (7) (2006) 603–632.
[15] K.Y. Lee, D.J. Mooney, Prog. Polym. Sci. 37 (1) (2012) 106–126.
[16] K.I. Draget, C. Taylor, Food Hydrocolloids 25 (2) (2011) 251–256.
[17] A. Johnston, et al., Curr. Opin. Colloid Interface Sci. 11 (4) (2006) 203–209.
[18] A.I. Bourbon, et al., COST Action FA0904, WG1 – Development of New Safe PNFP, Praga, Czech Republic, 2013.
[19] A. Agarwal, et al., J. Control. Release 128 (3) (2008) 255–260.
[20] B. Sun, et al., Langmuir 21 (23) (2005) 10763–10769.
[21] O. Mermut, C.J. Barrett, Analyst 126 (11) (2001) 1861–1865.
[22] K. Mladenovska, et al., Int. J. Pharmaceut. 342 (1-2) (2007) 124–136.
[23] A.C. Pinheiro, et al., J. Food Eng. 116 (3) (2013) 633–638.
[24] M.-L. De Temmerman, et al., Biomacromolecules 12 (4) (2011) 1283–1289.
[25] A.C. Pinheiro, et al., Carbohydr. Polym. 87 (2) (2012) 1081–1090.
[26] S. Dash, et al., Acta Poloniae Pharmaceut. 67 (3) (2010) 217–223.
[27] A.R. Berens, H.B. Hopfenberg, Polymer 19 (5) (1978) 489–496.
[28] A.C. Pinheiro, et al., Carbohydr. Polym. 115 (2015) 1–9.
[29] M.G. Carneiro-da-Cunha, et al., Carbohydr. Polym. 82 (1) (2010) 153–159.
[30] Q. Zhao, et al., J. Biomater. Sci. Polym. Ed. 17 (9) (2006) 997–1014.
[31] F. Caruso, Colloid Chemistry II, Springer, Berlin/Heidelberg, 2003, pp. 145–168.
[32] S. Honary, F. Zahir, Trop. J. Pharmaceut. Res. 12 (2) (2013) 265–273.
[33] A.K. Anal, et al., Colloids Surf. B: Biointerfaces 64 (1) (2008) 104–110.
[34] J. Zhou, et al., J. Colloid Interface Sci. 345 (2) (2010) 241–247.
[35] M. Corredig, N. Sharafbafi, E. Kristo, Food Hydrocolloids 25 (8) (2011) 1833–1841.
[36] K. Furusawa, S. Satou, Colloids Surf. A: Physicochem. Eng. Aspects 195 (1-3) (2001) 143–150.
[37] X. Gu, et al., Colloids Surf. B: Biointerfaces 108 (2013) 205–211.
[38] F. Caruso, R.A. Caruso, H. Möhwald, Chem. Mater. 11 (11) (1999) 3309–3314.
[39] W. Liu, et al., J. Mater. Sci. 46 (20) (2011) 6758–6765.
[40] G. Zhou, et al., Int. J. Nanomed. 8 (2013) 877–887.
[41] Z. Zhou, A.C. Anselmo, S. Mitragotri, Adv. Mater. (2013).
[42] D. Hu, et al., Int. J. Mol. Sci. 13 (5) (2012) 6454–6468.
[43] N.M. Mahajan, D.M. Sakarkar, A.S. Manmode, Int. J. Pharm. Pharmaceut. Sci. 3 (4) (2011) 208–214.
[44] A. Karewicz, J. Łegowik, M. Nowakowska, Polym. Bull. 66 (3) (2011) 433–443.
[45] C. Aguzzi, et al., Carbohydr. Polym. 85 (3) (2011) 638–644.
[46] M.A. Quintas, et al., 11th International Congress on Engineering and Food, 2011.
[47] X.-Y. Li, et al., J. Agric. Food Chem. 55 (8) (2007) 2911–2917.
[48] M. Kreuß, T. Strixner, U. Kulozik, Food Hydrocolloids 23 (7) (2009) 1818–1826.
[49] S. Ye, et al., J. Control. Release 112 (1) (2006) 79–87.
[50] E. Jager, et al., J. Biomed. Nanotechnol. 5 (1) (2009) 130–140.